Anal Bioanal Chem (2012) 403:2771–2783
DOI 10.1007/s00216-012-6062-z

ORIGINAL PAPER

Improved fluoroquinolone detection in ELISA through engineering of a broad-specific single-chain variable fragment binding simultaneously to 20 fluoroquinolones

Kai Wen · Greta Nölke · Stefan Schillberg · Zhanhui Wang · Suxia Zhang · Congming Wu · Haiyang Jiang · Hui Meng · Jianzhong Shen

Received: 8 February 2012 / Revised: 6 April 2012 / Accepted: 18 April 2012 / Published online: 2 May 2012

Abstract Fluoroquinolones (FQs) are a group of synthetic, broad-spectrum antibacterial agents. Due to its extensive use in animal industry and aquaculture, residues of these antibiotics and the emergence of bacteria resistant to FQs have become a major public health issue. To prepare a generic antibody capable of recognizing nearly all FQs, a single-chain variable fragment (scFv) was generated from the murine hybridoma cells C49H1 producing a FQ-specific monoclonal antibody. This scFv was characterized by indirect competitive enzyme-linked immunosorbent assay (ciELISA), and it showed identical binding properties to parental monoclonal antibody: it was capable of recognizing 17 of 20 targeted FQs below maximum residue limits, except for sarafloxacin (SAR), difloxacin (DIF), and trovafloxacin (TRO) which are highly concerned members in the FQs family. In order to broaden the specificity of this scFv to SAR and its analogues (DIF and TRO), protein homology modeling and antibody-ligands docking analysis were employed to identify the potential key amino acid residues involved in hapten antibody. A mutagenesis phage display library was generated by site directed mutagenesis randomizing five aminoacid residues in the third heavy-chain complementarity determining region. After one round of panning against biotinylated norfloxacin (NOR) and four rounds of panning against biotinylated SAR, scFv variants we screened showed up to 10-fold improved IC_{50} against SAR, DIF, and TRO in ciELISA while the specificity against other FQs was fully retained.

Keywords Fluoroquinolones · Molecular modeling · Phage display · scFv · Site-directed mutagenesis

Introduction

Fluoroquinolones (FQs) are a group of synthetic, broad-spectrum antibacterial agents derived from quinuolone nalidixic acid. Because of broad antibacterial spectrum and high antibacterial efficiency, FQs have become one of the most widely used antibacterial agents both in human medicine and livestock treatment. Although more than 20 different FQs derivatives have been synthesized and applied in practice since 1990s, the antibacterial mechanism of these FQs is almost the same: FQs inhibit the DNA replication in bacteria by inducing cleavage of bacterial DNA in the DNA-enzyme complexes of DNA gyrase and type IV topoisomerase, resulting in rapid bacterial death [1].

In recent years, FQs were extensively used in animal industry and aquaculture, not only for bacterial infection treatment but also for growth promotion and infection prevention. As a result of FQs abuse, residues of these drugs in animal tissue and the emergence of resistant bacteria strains to FQs have become a severe public health issue worldwide.

To control the hazards of residues in edible animals and to preserve the efficacy of FQs, strict maximal residue limits (MRLs) for FQs have been established in many countries

Electronic supplementary material The online version of this article (doi:10.1007/s00216-012-6062-z) contains supplementary material, which is available to authorized users.

K. Wen · Z. Wang · S. Zhang · C. Wu · H. Jiang · H. Meng · J. Shen (✉)
Yuanmingyuan West Road 2, Haidian District,
Beijing 100193, China
e-mail: sjz@cau.edu.cn

G. Nölke · S. Schillberg
Forckenbeckstraße 6,
Aachen 52074, Germany

and areas. In Europe, the Commission has set the approved administrative MRLs for FQs traces in animal tissues to 10-100 μg/kg.

Nowadays, the most commonly used analytical techniques for detection of FQs from food samples can be divided into three categories: instrumental, microbiological, and immunological methods. Generally, instrumental methods including liquid chromatography [2–4], mass spectrometry [5–7], and capillary electrophoresis [8–11] are accurate and sensitive but at the same time they are time consuming, solvent intensive, costly, and greatly rely on laboratory facilities as well as experimental skills. Therefore, these techniques are more suitable for confirmatory analysis than fast screening of a large number of food samples for FQs in field. Compared with instrumental methods, the microbiological tests used for screening of FQs are much more cost-effective and easier to operate, but they take usually about 20 h, and the sensitivity is much lower [12]. In contrast, immunological methods, especially the enzyme-linked immunosorbent assay (ELISA) have been widely applied in practice for screening of FQs because of its economic cost, high sensitivity and detection efficiency. In the last 20 years, many different immunoassay methods have been developed based on generation of FQs specific polyclonal and monoclonal antibody. Most of these methods only can recognize one single or minor class of FQs with high structure similarity [13, 14]. However, since over 20 FQs have been applied in practice, there is an emerging trend to develop a generic immunoassay that is capable of detecting all FQs derivatives in one single reaction. The fact that all FQs share a same core structure (Fig. 1) makes this possible. Current development of generic immunoassay is constrained by the availability of antibodies with appropriate affinity and broad-specificity characteristics. The ideal generic antibody is supposed to show similar cross reactivity to all members of a chemical group so can be exploited as broad selective receptors for development of rapid, low-cost screening analysis. In the recent years, several attempts have been made to obtain broad specificity antibodies enabling detection of up to 13 FQs in ELISA [15–18]. Furthermore, Wang and coworkers calculated and demonstrated the quantitative structure-activity relationship between antibody and various FQs by comparative molecular field analysis [18]. This study of structure-specificity relationship proved that molecular modeling is a promising tool for designing and optimization of immunogen. A new quantitative model based on field-overlapping coefficient of FQs had been developed by Cao et al. [19] to describe the conformational features of haptens and predict the specificity of antibodies. With the help of this model, Cao et al produced a polyclonal antibody capable of binding 13 FQs with similar affinity. Although these antibodies exhibited considerably high cross reactivity to many FQs, they still cannot recognize all the FQ members. The significant differences in structures of FQs made it very difficult to prepare a generic antibody with high homogenicity using conventional immunization techniques, which had been proved by previous researches. The inherit drawback of conventional antibody preparation technology is that the antibody can barely be optimized or evolved once it is generated. However, recombinant antibody and protein engineering technologies provide us a new solution to prepare generic antibodies. Leivo and coworkers [20] had utilized the error-prone mutagenesis and novel FQ derivatives to develop a broad-specificity antigen binding fragment recombinant antibody from a random mutant phage display library. In their research, the binding properties of parental sarafloxacin (SAR)-specific monoclonal antibody have been engineered successfully through random mutagenesis. The best mutant antibody they obtained was capable of recognizing seven of eight targeted FQs below MRLs. Despite of a great amount of efforts, a completely generic antibody is still not available. However, the previous

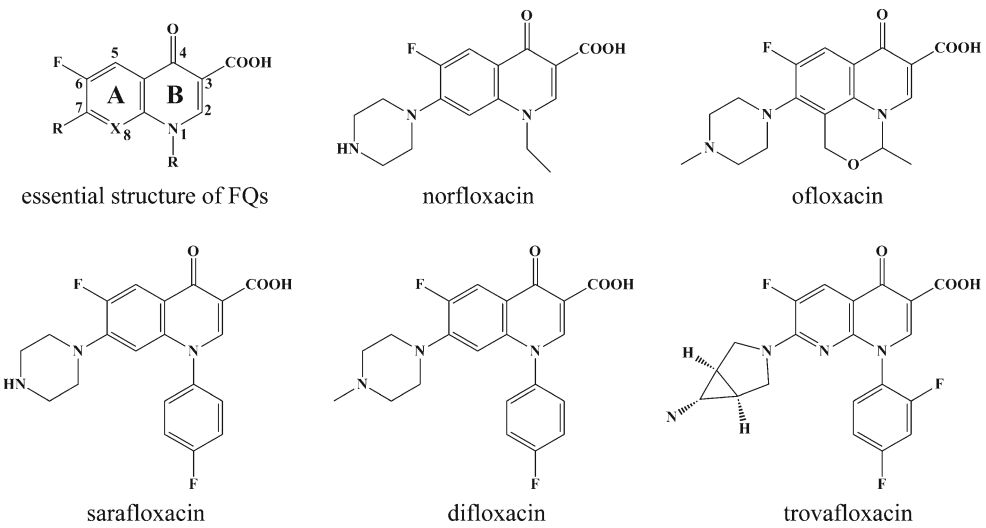

Fig. 1 The structures of representative FQs

studies showed that protein engineering associated with molecular modeling is a promising means to develop a broad-specificity antibody capable of binding all different FQs with a sufficient affinity for generic immunoassay.

The aim of our study was to prepare a broad-specificity recombinant antibody on basis of monoclonal antibody C49H1 previously generated in our lab so that we can develop a generic immunoassay capable of detecting a broader range of different FQs. To date, the antibody C49H1 is one of the best generic monoclonal antibodies available. It exhibited high cross-reactivity with 12 of 14 FQs [18], and only show poor binding to SAR and difloxacin. In the present study, the antibody C49H1 was cloned as a single-chain variable fragment (scFv) which retains the binding properties of parental monoclonal antibody (mAb). Molecular modeling was used to investigate the interactions between FQs and scFv. Based on the modeling information, we demonstrate the construction of a phage display library by site directed mutagenesis of third heavy-chain complementarity determining region (CDR H3) and report selection of scFv variants with improved binding activity to SAR, difloxacin (DIF), and trovafloxacin (TRO). The binding properties of selected scFv mutants against 20 FQs were successfully evaluated with indirect competitive enzyme-linked immunosorbent assay (ciELISA).

Materials and methods

Reagents and chemicals

Bovine serum albumin (BSA), ovalbumin (OVA), 3,3′,5,5′-tetramethylbenzidine (TMB), *N*-hydroxysuccinimide (NHS), and 1-ethyl-3-(3-dimethylaminopropyl) carbodiimide (EDC) were purchased from Sigma Chemical Co. (St. Louis, MO, USA). All other chemicals and solvents were of analytical grade or better and were obtained from Beijing Chemical Reagent Co. (Beijing, P.R.C.). EZ-Link Sulfo-NHS-LC-LC-Biotin reagent and high binding capacity biotin-binding plates were obtained from Thermo Scientific Pierce (Pierce Rockford, IL, USA). Streptavidin-coated magnetic nanoparticles (Dynabeads MyOne Streptavidin C1) and a magnetic separator (DYNAL MPC-S) were purchased from Invitrogen Dynal (AS, Oslo, Norway).

Standard solutions

Ciprofloxacin (CIP), danofloxacin (DAN), DIF hydrochloride, enoxacin (ENO), enrofloxacin (ENR), fleroxacin (FLER), amifloxacin (AMI), flumequine (FLU), levofloxacin (LEV), lomefloxacin hydrochloride (LOM), marbofloxacin (MAR), norfloxacin (NOR), ofloxacin (OFL), orbifloxacin (ORB), pazufloxacin (PAZ), pefloxacin-d5 (PEF), prulifloxacin (PRU), SAR hydrochloride trihydrate, sparfloxacin (SPA), and TRO mesylate analytical standards were purchased from VETRANAL® Fluka (Sigma-Aldrich, St. Louis, MO, USA). Standard stock solutions (100 μg mL^{-1}) of antibiotics were prepared by dissolving an appropriate amount of each standard in 0.03 M sodium hydroxide. The individual stock solutions were stored at 4 °C in amber glass bottles and were stable for at least 3 months. Working standard of each antibiotic was prepared by diluting the stock solution in assay buffer.

Microbiology reagents

All the medium used in this study were prepared as described in the literature [21]. Dulbecco's modified Eagle's media used for cell culture was obtained from Huamei (Beijing, P.R.C.). *Escherichia coli K12* strain XL1-Blue was purchased from Stratagene (La Jolla, CA, USA). RV308 strains were obtained from ATCC. Tetracycline, chloramphenicol, and kanamycin (>99 % pure) were obtained from Sigma-Aldrich (St. Louis, MO, USA). M13KO7 helper phage (Kan^R) and restriction enzymes used in cloning and library construction were purchased from New England Biolabs (Beijing, P.R.C.). Isopropyl β-D-1-Thiogalactopyranoside (IPTG) was obtained from Promega (Madison, WI, USA). The vector pAK100 and pJB33 used for phage display and scFv expression were obtained as gifts from the laboratory of Andreas Plückthun (Biochemisches Institut, Universität Zürich, Switzerland). Monoclonal cell-line C4A9H1 was established previously in our laboratory [18]. The anti-*c-myc* 9E10 antibody and the peroxidase-conjugated goat antimouse IgG (IgG–HRP) was obtained from Jackson ImmunoResearch Laboratories, Inc. (West Grove, PA, USA).

Preparation of OVA-conjugated NOR

The coating antigens were prepared by conjugating (NOR) to OVA using the NHS ester method previously described [22] with modifications: the hapten (15 mg) was dissolved in DMF (5 mL), and the solution was cooled with cold ethanol (4 °C). NHS (20 mg) and EDC (20 mg) were added to the hapten solution, and the mixture was stirred at room temperature (RT) overnight. OVA (15 mg) was dissolved in 5 mL of carbonate buffer (pH 8.0) and added dropwise to the active NHS solution with continuous stirring and further stirred at RT for 4 h. The hapten–OVA conjugates were dialyzed against PBS (pH 7.0) at 4 °C for 72 h, and then characterized with UV–vis spectrometry.

Biotinylation of NOR and SAR

Biotinylation of NOR and SAR was performed as described previously [20] with modifications using EZ-Link Sulfo-

NHS-LC-LC-Biotin reagent (Thermo Scientific Pierce): NOR(2 mg, 6.25 μmol) or SAR(2 mg, 5.2 μmol) and sulfo-NHS-LC-LC-biotin linker (8 mg, 12 μmol) were dissolved in 1 mL of PBS and stirred at RT for 120 min. The liquid in reaction mixture was evaporated with lyophilization, and the precipitate was dissolved in 50:50 (*v*/*v*) H_2O/acetonitrile. The products were analyzed with MALDI-TOF MS, where the main peak was detected at $[M+H^+]=772.6$. The biotin was conjugated to the secondary amine in the piperazinyl of NOR or SAR in the final products.

Cloning of mabC4A9H1 to scFv format

mAb isotype was determined with mouse mAb isotyping kit (Pierce). Total RNA was isolated from hybridoma C4A9H1 cells using the Qiagen RNeasy Mini Kit and QIAshredder (Qiagen, Shanghai, P.R.C.) as instructed by the manufacturer. The complementary DNA (cDNA) was synthesized with the SuperScript™ First-Strand Synthesis System for RT-PCR (Invitrogen, Shanghai, P.R.C.) following the oligo $(dt)_{20}$ protocol of kit. After a RACE external primer specific tag sequence was added onto the 3′ end of cDNA using T4 ssRNA Ligase (New England Biolabs, Beijing, P.R.C.), heavy-chain (HC) fd gene and whole lambda light-chain (LC) gene were amplified with the RACE internal and external primers (Electronic Supplementary Material Table S1) using Expand High Fidelity polymerase chain reaction (PCR) system (Roche, Beijing, P.R.C.) as instructed by the manufacturer. The purified PCR products (HC and LC gene) were separately cloned into the pCR®2.1-TOPO vector (Invitrogen) according to the manufacturer's instructions and. Several individual clones of HC and LC gene were sequenced, and the correct sequences were deduced and identified by comparison to the corresponding germline gene sequences from the international ImMunoGeneTics database (IMGT). A full-length scFv gene in 5′-V_L-$(Gly_4Ser)_4$-V_H-3′ orientation followed by c-myc tag was synthesized by GenScript Corporation (Piscataway, NJ, USA) using preferred codon by *E. coli*. Afterward, the synthesized scFv gene was cloned to the pJB33 vector [23] using the introduced *Sfi*I sites and transformed into *E. coli* RV308. The transformants were selected on Luria-Bertani (LB) plates supplemented with 30 μg/mL chloramphenicol and incubated overnight at 37 °C. Plasmids were extracted from the culture made from the transformants and analyzed by restriction enzyme digestions and electrophoresis. The plasmids containing the fragments of right sizes were confirmed by DNA sequencing.

Expression, purification, and characterization of scFv

To express soluble scFv, single colonies harboring the plasmid encoding the respective scFv fragment were incubated overnight at 37 °C with shaking (200 rpm) in 10 mL Super Broth medium (SB medium) containing chloramphenicol until the OD_{600nm} of the cultures reached 0.5. IPTG was added to a final concentration of 100 μM, and growth was continued for 4 h (26 °C, 250 rpm). The cells were harvested by centrifugation and resuspended thoroughly in 2 mL precooled extraction buffer (30 mM Tris–HCl, 2 mM EDTA, 20 % (*w*/*v*) sucrose, and 100 μg/ml lysozyme, Sigma-Aldrich). The suspensions were stored on ice for 30 min. Cell debris was removed by centrifugation, and the supernatant was collected and dialyzed (12- to 14-kDa molecular weight cut-off) against 4 L PBS and stored at 4 °C.

The purification of scFv was carried out by immobilized metal affinity chromatography (IMAC) using a 5-mL HisTrap™ HP column (GE Healthcare, Beijing, P.R.C.) according to the manufacturer's instructions. For detection, a UV detector at a wavelength of 280 nm was used. Each peak was collected separately and checked by SDS-PAGE, immunoblot, and ciELISA.

Molecular modeling and docking of scFv and FQs

Homology modeling is the most reliable computational method for predicting protein structure from its sequence. Discovery Studio 2.5 (DS 2.5, Accelrys Software Inc., San Diego, CA, USA) computer program was used to construct the homology model of scFv. Antibody 10e5 (PDB code: 2VC2) [24] and antibody N1g9 (PDB code: 1NGQ) [25] retrieved from National Center for Biotechnology Information (NCBI) by BLAST were used as structure alignment templates for V_H and V_L, respectively. 10 homology models of V_H and V_L were created and refined independently using Modeler block in DS 2.5. Probability density function (PDF) Total Energy, PDF Physical Energy and DOPE Score Discrete Optimized Protein Energy (DOPE) scores for each model were calculated for models evaluation. To build the entire Fv domain model, the V_H and V_L models with highest DOPE scores were selected and superimposed onto corresponding domains in PDB structure of antibody 9B1 [26] by performing a least squares fit on the backbone atoms of the conserved framework residues. Except for CDR H3, all the 5 of 6 CDR loops in the Fv domain model were identified against antibody database and reconstructed using the Model Antibody Loops protocol and refined by Loops refinement protocol in DS 2.5. As the most critical and variable part of the Fv domain, the CDR H3 loop was reconstructed and refined with CHARMm, LOOPER, and CHIROTOR blocks using de novo physics based methods [27] to break the bias inherited from templates and side chains of surrounding amino acid residues. Finally, the whole Fv model was refined by energy minimization with 40 iterations of Steepest Descent-algorithm and 100 iterations of Conjugate Gradients-algorithm. The final Fv model

was examined under Ramachandran plot and validated using Verify protein (Profiles-3D) protocol in DS 2.5.

For protein-ligand docking, 3D structures of FQs (NOR and SAR) were retrieved from NCBI-PubChem compound database and initialized as ligand molecules (valid ionization, removing duplicates, enumerating isomers and tautomers, and generating reasonable 3D conformation) with the DS 2.5 tool "Ligand Preparation." All the possible torsion angles in ligand molecules were set to rotate freely. The Fv model was set as receptor and six CDR loops were defined as sphere of binding site (sphere radius, 15 Å; sphere center, 48.876, 57.138, and 11.4 for *x*-, *y*-, and *z*-coordinates). The flexible molecular docking of FQs onto scFv model was accomplished using automated Genetic Optimization for Ligand Docking (GOLD) protocol in DS 2.5 with high predictive accuracy Generic Algorithm (GA) parameters. For each FQ ligand, ten ligand poses were generated from docking experiment and evaluated with GOLDscore function taking into account factors such as H-bonding energy, van der Waals energy and ligand torsion strain. The further analysis of all the ligand poses and receptor–ligand interactions were performed using Analyze binding site tools in DS 2.5.The top ranked ligand poses for NOR and SAR were used for further study.

Site-directed mutagenesis library

On basis of molecular modeling of scFv, five amino acid residues in the CDR H3 were selected for site-directed mutagenesis and Oligo-directed mutagenesis strategy was used to randomize each selected amino acid residue. The scFv gene was mutated using Expand High Fidelity PCR System (Roche) with primer A and B (Table S1 in the Electronic supplementary material ESM) producing 50 % probability of retention of wild-type amino acid at each position. Whole scFv gene containing restricted enzyme sites was amplified with primer A and C (Table S1 in the ESM). Two micrograms of purified PCR product was cloned into pAK100 phagemid vector (molar ratio of vector to insert, 1:5) using the introduced *Sfi*I sites. The ligation reactions were purified with ethanol precipitation and electroporated to electrocompetent *E. coli* XL1-Blue cells in 10 separate electroporations, yielding approximate 2.4×10^8 transformants. The transformed cells was regenerated in 10 mL SOC medium at 37 °C and 150 rpm for 1 h, and then culture was plated on 2×YT agar plates containing 1 % (*w*/*v*) glucose, chloramphenicol, tetracycline and incubate overnight at 37 °C. Several single colonies were picked up from plate and sequenced to evaluate the diversity of library. The remaining colonies on the agar plate were scraped off in 5 ml 2×YT containing 30 % (*v*/*v*) glycerol and the cell density of this suspension was estimated by OD_{600nm} value. 5×10^9 cells from this suspension were inoculated in 100 mL 2×YT medium and cultivated at 37 °C until OD_{600nm} reached 0.8. Then 10 mL of this culture was infected with 10^{11} pfu of M13KO7 helper phage for 15 min at 37 °C without shaking. Cells were harvested by centrifugation (3,000×*g*, 10 min, 4 °C) and resuspended in 50 mL of 2×YT medium containing tetracycline and chloramphenicol. After 2 h of growth at 37 °C and 200 rpm, IPTG (100 μM) and kanamycin (75 μg/mL) were added to the culture. Phage production was continued overnight (26 °C, 250 rpm). The bacteria was pelleted by centrifugation and the phage particles in supernatant were precipitated twice with a solution containing 5 % (*w*/*v*) polyethylene glycol 8000 and 4 % (*w*/*v*) NaCl. Phages were finally dissolved in 200 μL PBS containing 1 % (*w*/*v*) BSA. The purified primary phage library was stored at 4 °C.

Enrichment and screening of phage library

The phage library was enriched with streptavidin-coated magnetic C1MyOne nanoparticles as described previously [20]. Prior to each panning round, the PBS solution of 1.0×10^{12} purified phage particles displaying scFv was blocked with 1 % (*w*/*v*) BSA in PBS at RT for 30 min followed by incubation in the streptavidin-coated microtiter wells for 1 h to remove the unspecific and streptavidin-specific binders. These preselected phages and biotinylated hapten were incubated with slow shaking for 2 h at RT. Afterward, 1×10^5 streptavidin-magnetic beads were added to the phage-antigen mix and incubate on rotator at RT for 15 min. Beads were collected with an MPC-S bead collector (Dynal) and washed three times with PBST—0.05 buffer (PBS containing 0.05 % (*v*/*v*) Tween 20, pH 7.5). Phages were eluted by HCl/glycine buffer in the first panning round and by competition with free SAR solution of different concentration for 1 h at RT in following four panning rounds. The eluted phage was purified on a PD-10 desalting column (GE Healthcare) following manufacturer's instruction to remove the antibiotic competitor and used to infect 5 mL of *E. coli* XL1-Blue cells in logarithmic growth phase (OD_{600nm}, ≈0.5) for 30 min at 37 °C. The infected culture was diluted to 50 mL and used to prepare phage stock as described earlier. Enrichment of the library was confirmed and estimated by plated dilutions from the infection step by comparison with non-antigen-containing selections and polyclonal phage ELISA.

After five rounds of panning, 20 single colonies were selected from the output plates to propagate monoclonal phages following the same protocol for preparation of primary phage library stock. The clones showing improved affinity to SAR in monoclonal phage ciELISA were selected for further study.

Characterization of active clones

Five scFv genes from selected active clones were subcloned to pJB33 with *Sfi*I. The expression and purification were

performed as described above. The cross-reactivity profiles of the active scFv mutants against various FQs were determined by ciELISA. The buffers and solutions used in ciELISA were prepared as described [18]. The ciELISA was carried out as follow: Costar high-binding enzyme immunoassay 96-well plates (Corning Inc., Shanghai, P.R.C.) were coated with NOR-OVA conjugate at 4 °C overnight. The plates were washed three times with washing buffer, and then blocked with blocking buffer (300 μL/well) at RT for 1 h. For competition, 50 μL of a standard solutions of various concentrations and 50 μL of scFv (1.7 μg/mL in PBS) were simultaneously added to each coated well. Then, the plates were incubated for 1 h at RT followed by a three times washing as described above. Anti-*c-myc* monoclonal antibody 9E10 (1:5,000 in PBS) and goat antimouse IgG-HRP conjugate (1:5,000 in PBS) were simultaneously added to wells and incubated at RT for 1 h. After three times plates washing, the substrate solution was added and incubated at RT for 30 min before the enzymatic reaction was stopped by adding 2 M H_2SO_4 (100 μL/well). The absorbance (A) of each well was measured at 490 nm by the ELISA plate reader. The four parameter logistic nonlinear regression model was used to fit the standard curves and analysis each IC_{50} value of competitors. The cross-reactivity values were calculated by dividing the IC_{50} value of NOR by the IC_{50} of the tested analogues and multiplied by 100.

Results and discussion

Generation and characterization of murine scFv

Today, many different methods have been successfully used in amplification of the hybridoma V genes. The V region primers PCR, especially if using diverse primer sets had been proved efficient for this purpose [28–30]. However, there are several potential pitfalls in V region primers PCR. Mutations in the 5′ or 3′ ends of the V genes may prevent amplification. Moreover, universal V region primers can introduce mutations which may reduce the stability, production yield, and antigen affinity of the scFv encoded by these amplified V gene [31]. Besides these, in the hybridoma, the presence of other V genes from nonproductive rearrangements or other fused spleen cells are preferentially amplified, which result in multiple functional, as well as nonfunctional V genes. In this situation, an alternative to V gene PCR is to amplify the complete V gene, including 5′-untranslated region, leader sequence, and a part of the constant region using rapid amplification of cDNA ends (RACE). In this study, the isotype of the monoclonal antibody C4A9H1 HC and LC were determined as IgG1 and Lambda, respectively. This isotype information provided sequence knowledge of the constant region, which was used to design the internal primer. Using the RACE external tag labeled cDNA as PCR template, HC fd region and whole lambda LC were successfully amplified with RACE external and internal primers. Based on the deduced amino acid sequences and protein BLAST analysis, the correct V gene sequences were identified and assembled in 5′-VL-$(Gly_4Ser)_4$-VH-3′ format to construct the full-length scFv gene.

For high efficiency periplasmic expression of soluble scFv in *Escherichia coli*, the assembled scFv gene was cloned into an enhanced expression vector pJB33 [32] after optimizations of codon usage bias, GC content, mRNA secondary structure and other critical parameters. The scFv was produced in *E. coli* strain RV308 and purified by IMAC (Fig. 2). In the expression of soluble scFv, the higher IPTG concentration (1 mM) used to induce *E. coli* culture led to larger total amount of expressed soluble scFv as well as relatively more serious leakiness of scFv from periplasm into medium. Therefore, the amount of scFv in periplasmic extract did not show any obvious improvement along with the increasing IPTG concentration.

The binding property of purified scFv was investigated in ciELISA using NOR-OVA conjugate as antigen coated to the microtiter plate and various FQs derivatives as analyte competitors. Table 1 shows the IC_{50} values and cross-reactivity profile of scFvC4A9H1 and the parental mab-C4A9H1 to the 20 FQs. The scFvC4A9H1 exhibited high cross reactivity (CR) to nearly all FQs except for the derivatives possessing a fluorophenyl ring at position 1 (SAR, DIF, TRO), which is consistent with the CR profile of mAb. Both mabC4A9H1 and scFvC4A9H1 showed high CR (more than 50 %) to the FQs (CIP, ENR, NOR, PEF, DAN, LEV, OFL, and AMI) with high structural similarity to NOR which has been used for the generation of mAbC49H1. All of these FQs derivatives possess a piperazinyl at position 7 and small alkane substitutions at position

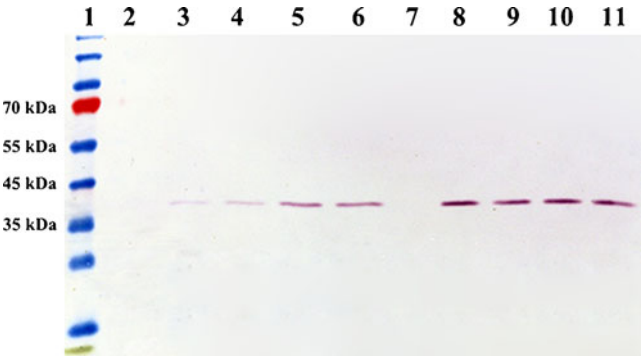

Fig. 2 Immunoblotting analysis of soluble scFv. *Lanes 2–6*, the medium fractions of the cultures induced with 0, 0.25, 0.5, 0.75, and 1.0 mM IPTG, respectively; *lanes 7–11*, the periplasmic extract from the cultures induced with 0, 0.25, 0.5, 0.75, and 1.0 mM IPTG, respectively; *lane 1*, prestained protein ladder marker. All the samples are normalized to the same OD_{600} of the original culture

Table 1 Cross-reactivity profile and IC_{50} values to FQs

FQs	Parental mAb		scFvC4A9H1		scFvC4A9H1_mut1		scFvC4A9H1_mut2		scFvC4A9H1_mut3		scFvC4A9H1_mut4		scFvC4A9H1_mut5	
	IC_{50} (ng/mL)	CR %	IC_{50} (ng/mL)	CR %	IC_{50} (ng/mL)	CR %	IC_{50} (ng/mL)	CR %	IC_{50} (ng/mL)	CR %	IC_{50} (ng/mL)	CR %	IC_{50} (ng/mL)	CR %
CIP	0.25	128.00	0.27	111.11	0.31	119.35	0.25	126.48	0.28	114.41	0.60	93.08	0.47	113.16
ENR	0.28	114.29	0.29	103.45	0.34	108.82	0.31	102.62	0.31	103.97	0.58	95.93	0.54	98.51
NOR	0.32	100.00	0.30	100.00	0.37	100.00	0.32	100.00	0.32	100.00	0.56	100.00	0.53	100.00
PEF	0.36	88.89	0.32	93.75	0.34	108.82	0.35	91.03	0.33	98.89	0.53	105.71	0.56	95.73
DAN	0.45	71.11	0.46	65.22	0.51	72.55	0.46	69.40	0.51	63.70	0.71	78.30	0.82	64.64
LEV	0.46	69.57	0.46	65.22	0.53	69.81	0.44	72.80	0.46	70.56	0.87	64.17	0.79	67.17
OFL	0.47	68.09	0.48	62.50	0.55	67.27	0.50	63.29	0.50	63.98	0.86	65.17	0.87	60.79
AMI	0.48	66.67	0.49	61.22	0.55	67.27	0.45	71.16	0.50	64.96	1.22	45.68	0.81	65.29
ENO	0.53	60.38	0.51	58.82	0.62	59.68	0.48	66.19	0.49	65.35	0.88	63.15	0.81	65.79
ORB	0.57	56.14	0.55	54.55	0.60	61.67	0.59	54.18	0.50	64.40	1.10	50.79	1.00	52.90
FLER	0.58	55.17	0.59	50.85	0.65	56.92	0.55	57.73	0.63	51.24	0.91	61.33	1.17	45.28
SPA	0.58	55.17	0.60	50.00	0.60	61.67	0.59	54.35	0.65	49.92	1.05	53.07	1.14	46.49
MAR	0.59	54.24	0.55	54.55	0.67	55.22	0.54	58.70	0.53	60.77	1.05	53.15	1.05	50.52
LOM	0.61	52.46	0.60	50.00	0.65	56.92	0.58	54.84	0.59	55.07	1.04	53.80	1.09	48.65
FLU	0.67	47.76	0.65	46.15	1.34	27.61	1.45	21.89	1.40	22.98	356	0.16	324	0.16
PAZ	0.69	46.38	0.68	44.12	1.41	26.24	1.41	22.52	1.49	21.56	332	0.17	310	0.17
PRU	5.30	6.04	5.80	5.17	9.70	3.81	10.46	3.04	8.91	3.62	2,361	0.02	2,400	0.02
SAR	257	0.12	265	0.11	24.50	1.51	26.78	1.19	25.12	1.28	48.15	1.16	45.13	1.18
DIF	266	0.12	278	0.11	25.20	1.47	24.90	1.28	22.74	1.42	48.23	1.16	47.81	1.11
TRO	871	0.04	1,023	0.03	89.20	0.41	84.61	0.38	94.46	0.34	142.28	0.39	153.47	0.35

1. The minor structural differences at positions 1 and 7 in these FQs only have a limited impact on the conformation of these FQs as already shown in previous study [18, 19]. Lower but similar CR ranging from 36 to 47 % were observed with both mabC4A9H1 and scFvC4A9H1 against ENO, ORB, FLER, SPA, MAR, LOM, FLU, and PAZ. These FQs comprise another important group in the FQs family: they all possess a ring structure or a significant ring-like conformation around positions 1 and 8, which may be responsible for the decreased CR compared with NOR [18]. Similar to the mAb, the scFv has poor IC_{50} values against SAR, DIF and TRO. This low cross-reactivity is mainly explained by the molecular conformation changes of these FQs group compared with NOR. The large fluorophenyl at position 1 in these FQs formed a plane that lies perpendicular to the plane of rings A and B. The poor binding affinity exhibited by scFvC4A9H1 and mAbC4A9H1 is the result of this steric hindrance [18].

This CR consistency between scFvC4A9H1 and parental mAbC4A9H1 indicated that the scFv molecule fully inherited binding characteristics from mAb, and, therefore this scFv was a promising candidate for further scFv engineering.

Molecular modeling and FQs docking

Once the mAbC4A9H1 was cloned successfully into the scFv format, the sequence information of the V regions could be used to develop the molecular model and guide the in vitro engineering of scFvC4A9H1. Although homology modeling is the most efficient and reliable computational method for predicting protein structure from its sequence, the conformation computation of six CDRs is always the most challenging part in antibody modeling. In this study, fortunately, the protein alignment templates of 100 % similarity to the CDR L1, L2, L3, and H1 of scFvC4A9H1, respectively, were identified from PDB, and the best retrieved template to CDR H2 showed 83.3 % similarity. Based on these templates of good homology, high quality models for five of six CDRs of scFvC4A9H1, except H3, were constructed using the MODLLER and LOOPER blocks in DS 2.5 software (Fig. 5a). The long CDR H3 consisted of 14 amino acids in scFvC4A9H1 exhibited very high uniqueness and the best template retrieved from PDB showed only 42.9 % similarity to it. Therefore, the de novo physics based method was used to reconstruct the loop ignoring its starting conformation, and thus breaking the bias inherited from the initial template [27]. The analysis of the Ramachandran plot showed that 96 % amino acid residues of the final model are present in allowed region (Fig. S1 in the ESM). DS 2.5 Profiles-3D verify score for the final Fv model was 117.98 and higher than the verify expected high score (105.81), confirming the reliability of the modeled structure (Fig. S2 in the ESM).

Since the parental mAb was raised against NOR-BSA conjugate [18] and the structure of NOR most closely mimics the common moiety in all FQs, NOR was used in our docking study to investigate the binding site and the key contact residues in scFv-FQs complex. On the other hand, as the target compound of affinity engineering and the representative of FQs possessing a big fluorophenyl at position 1 (Fig. 1), SAR was also docked into the scFv model to identify the important residues that possibly affect the hapten binding. Ten ligand poses were generated for NOR and SAR, respectively, under pre-defined GOLD algorithm settings delivering high predictive accuracy. The evaluation of generated NOR poses displayed a series of ligand fitness GOLD score ranging from 23.136 to 38.4559 while the corresponding score for SAR poses varied from 29.283 to34.927 (Table S2 in the ESM). The NOR/SAR-scFv model containing top ranked ligand pose were selected for further study and shown in Fig. 5. The modeling of interaction between scFv and NOR or SAR, respectively, showed that scFvC4A9H1 recognizes and binds NOR (Fig. 3b) or SAR (Fig. 3d), respectively, by a narrow "cavity-groove" formed by five of CDR loops, H1, H2, H3, L1, and L3 while the CDR L2 was located on the outer surface and did not contact ligand directly (Fig. 3). The carboxyl group at position 3 of FQs common moiety was buried deeply in the small cavity of ~6 Å deep and ~3 Å diameter, where it is surrounded by positively charged residues and a hydrogen bond was observed between CDR H2 Arg 58 (numbered according to Kabat numbering system [33])and the carboxyl oxygen atom (distance, ~2 Å). In both models of SAR and NOR, the ring A and ring B lied in a same plane and were bound in the groove formed by ArgH50, TrpL91, and AsnL94 (Fig. 3). In this shallow binding groove, a stable contacts network composed of four π-cation interactions was observed between π systems from rings A and ring B and the cations provided by protonated side chain of ArgH50 while a relatively weak π–σ interaction was formed by ring B and the hydrogen atom of phenyl in the L/Trp91 side chain. In addition, the ring A was also bound by residue SerH97 *via* a hydrogen bond between the fluorine atom and the hydroxyl hydrogen atom in the serine side chain. All these short contacts between ligand and receptor were observed in both models of SAR and NOR, but the distances of these contacts in NOR model were significantly shorter, generally meaning stronger interaction than corresponding contacts in SAR, which was perceived as the result of steric hindrance from perpendicular plane (against rings A and ring B) formed by the large fluorophenyl substitution at position 1 in SAR. Furthermore, this steric hindrance also significantly affected the recognition and binding of scFvC4A9H1 to piperazinyl ring at position 7, another important common structure of NOR, SAR, and most of other FQs. In the SAR docked model, the slightly increased

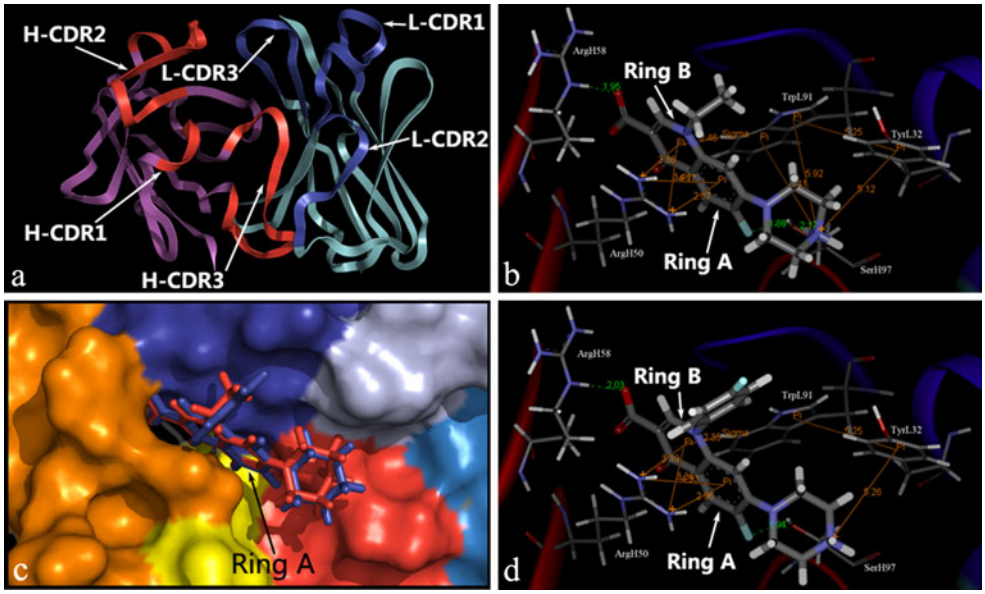

Fig. 3 Modeling of the interaction between scFvC4A9H1 and FQs. **a** Cα ribbon diagram of homology model of Fv domain; **b** interactions between NOR and scFv binding site; **c** the superimposition of NOR-scFvC4A9H1 and SAR-scFvC4A9H1 complexes. CDR H1, H2, and H3 were shown as solvent accessible surface in *yellow*, *orange*, and *red*, respectively, and CDR L1, L2, and L3 were shown in *light blue*, *sky blue*, and *deep blue*, respectively, the NOR and SAR molecules were shown as *sticks in red* and *blue*, respectively; **d** interactions between SAR and scFvC4A9H1 binding site. The predicted interactions are shown as *straight lines*. This figure was generated with Pymol and DS 2.5

distance between ligand and active binding residues caused by the fluorophenyl group led to the dramatic decrease of interaction strength. Only a weak π–cation interaction (distance, ~5.26 Å) was observed between the protonated distal piperazinyl nitrogen atom and the aromatic ring in the TyrL32 side chain. In the NOR docked model, by contrast, more and stronger interactions were found around the piperazinyl group. In the absence of large fluorophenyl substitution at position 1, the piperazinyl ring formed a "boat conformation" and the distal piperazinyl nitrogen atom bent towards the side chain of SerH97. Compared with the "chair conformation" of the piperazinyl ring in SAR (Fig. 3d), the protonated distal nitrogen atom was much closer to the oxygen atom of the hydroxyl in the SerH97 side chain, and so a strong hydrogen bond was formed here. Furthermore, the bending down nitrogen atom in this "boat conformation" also provided a cation center for the surrounding aromatic rings and evoked a simple and stable π–cation interaction network among nitrogen cation, TyrL32 and TrpL91 (Fig. 3).

All of these shorter contacts and stronger interactions between NOR and scFvC4A9H1 discussed above explained the hundreds times higher affinity of scFvC4A9H1 to NOR. Since the recognition of ring A, ring B and carboxyl group in the SAR-scFvC4A9H1 interaction were almost the same as those in the NOR-scFvC4A9H1 complexes, the interactions between piperazinyl ring and binding site were considered as the decisive factor for the improvement of the affinity to SAR. As shown in the docking models, the SerH97 located in CDR H3 was a important residue in the recognition of the piperazinyl ring. As described above, in the NOR-scFvC4A9H1 complex, compared with SAR-scFvC4A9H1 complex, there was one more hydrogen bond formed between the end nitrogen atom of the piperazinyl ring and the SerH97 side chain due to the shorter distance between them. Given the fact that it is quite difficult to shorten the distance between the corresponding atoms in the SAR-scFvC4A9H1 complex by directly changing or modifying the piperazinyl conformation, the mutagenesis in CDR H3 N-terminal residues under the piperazinyl seems to be a rational and promising alternate approach to improve the recognition of piperazinyl ring in SAR. On basis of this interaction analysis, the first five N-terminal residues of the CDR H3 in scFvC4A9H1 were selected as key positions for proceeding mutagenesis research.

Construction and screening of mutagenesis library

For in vitro antibody affinity maturation, site-directed mutagenesis in CDR loops combined with phage display has been proved to be one of the most effective means to increase antibody affinity [34, 35]. However, many CDR residues, especially the CDR H3 residues play the dominant roles in interactions with antigen. The mutagenesis targeted to these residues in CDR loops can result in dramatically decreased affinity to antigen. In this paper, on the basis of

docking study, the first five N-terminal residues of CDR H3 loop were considered as key positions to improve binding to the piperazinyl group and so were selected as targets of site directed mutagenesis. To improve the effective capacity of mutagenesis library, oligonucleotides primers (Table S1 in the ESM) containing tuned NNS codons biased for wild-type residues were used to randomize each selected position. These biased degenerated primers can produce approximately 50 % wild-type amino acid at each randomized position. Thus, the number of non-viable structures and non-active clones were minimized during the induction of mutations, which was useful to improve the effective capacity of mutant library.

Mutated scFv DNAs were purified and cloned into a pAK100 phagemid vector. The scFv mutants were produced as filamentous phage coat protein III fusions from this vector, enabling phage display. After electroporation into *E. coli* XL1-Blue cells, a mutagenesis library containing ~2.4×10^8 independent colonies was constructed. The sequencing results of 40 randomly picked individual clones showed a very low self-ligation background and a good diversity of mutated sites (every sequence of these 40 individual clones was different from others). In order to obtain the generic FQs binders with improved affinity to the free hapten SAR, a specific library selection strategy using alternated antigen (biotinylated NOR and biotinylated SAR) for panning and competitive elution (using free SAR as competitor to elute the binders) was employed. Moreover, a solution- phase panning procedure was performed to ensure the selection of scFvs based on binding affinity or binding kinetics rather than avidity [36]. This is especially important because some low affinity mutants in scFv library may spontaneously dimerize in a sequence dependent manner, and so exhibiting higher avidity than the monomeric scFvs [37]. In the first panning round, biotinylated NOR was used as antigen to enrich NOR specific binders in the library, and to retain the binding property of wild-type scFv. In four subsequent panning rounds, this preliminary enriched library was selected on SAR and competitively eluted with SAR solution of decreased concentration at each round from 10 to 0.01 μg/mL (10-fold decrease in each round). After each panning round, a part of the eluted phages were titered to determine the amount of output phages (the output values from the first to the fifth round were 7.3×10^5, 1.4×10^5, 6.1×10^5, 1.1×10^6, and 6.2×10^6, respectively), and the remained phages were used to infect XL1-Blue cells for amplification. Because of the change of the panning antigen in the second round, the amount of output phage reduced significantly to 1.4×10^5 in contrast to the first round (7.3×10^5). However, the gradually increasing output of library from 1.4×10^5 to 6.2×10^6 was observed during subsequent panning rounds on SAR, indicating that specific mutants were enriched successfully in library even after the change of the panning antigen. The library enrichment was also monitored by polyclonal phage ciELISA using amplified phage and NOR-OVA conjugate after each panning round. The ciELISA was performed as described above, and the amount of amplified phage from each round used in ciELISA was normalized to yield an absorption signal around 1.5 at 490 nm. The calculated IC_{50} values of polyclonal phages displaying scFvs to free SAR are shown in Fig. 4. Both the decreasing IC_{50} values and the amount of phages used to produce the same signal in ciELISA suggested that the binders with improved affinity to free SAR were enriched significantly. A minor decrease of IC_{50} was observed after the first panning round on NOR, even without any selection on SAR, which was considered as the result of elimination of nonspecific binders in the library. During subsequent panning on SAR combined with SAR competitive elution, the IC_{50} reduced gradually from 312 to 30 ng/mL. However, the decrease of IC_{50} after fourth and fifth round became much slower, which reflected the limit of this mutagenesis library. Although three additional selection rounds were performed, the IC_{50} values of amplified phage did not show any significant change (data not shown). Therefore, output clones from the fifth panning round were selected for further characterization

Analysis of positive mutants

After five panning rounds, five different mutants (scFvC4A9H1_mut1, scFvC4A9H1_mut2, scFvC4A9H1_mut3, scFvC4A9H1_mut4, and scFvC4A9H1_mut5) showing similar or improved affinity to SAR and its analogues (DIF and TRO) were obtained from site-directed CDR H3 mutagenesis library. The five scFv DNAs were sequenced and the corresponding amino acid sequences deduced to identify mutated amino acid positions (Table 2). Moreover, the scFvC4A9H1_mut1 to scFvC4A9H1_mut5 were produced in *E. coli*, affinity purified and tested in ciELISA to determine binding specificities to the selected 20 FQs (Fig. 5; Table 1). According to the amino acid sequence

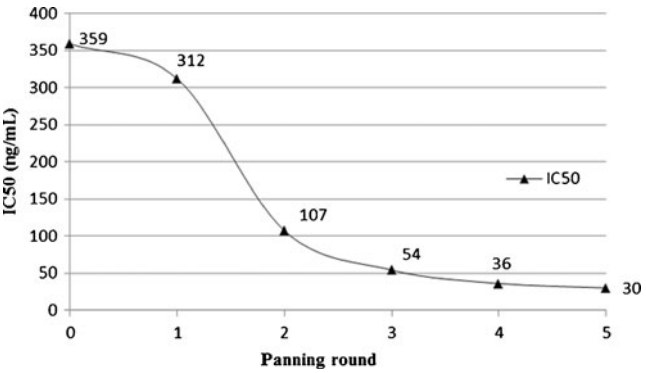

Fig. 4 IC_{50} of polyclonal phage displayed scFv to SAR from each panning round

Table 2 Mutant sequences

Mutants	H95	H96	H97	H98	H99
scFvC4A9H1	Ala	Leu	Ser	Leu	Tyr
scFvC4A9H1_mut1	Ala	Gly	Ser	Ala	Tyr
scFvC4A9H1_mut2	Gly	Gly	Ser	Ala	Tyr
scFvC4A9H1_mut3	Gly	Ala	Ser	Gly	Tyr
scFvC4A9H1_mut4	Ala	Gly	Arg	Gly	Gln
scFvC4A9H1_mut5	Ser	Ala	Arg	Gly	Gln

Residues discussed were numbered according to Kabat nomenclature system [33]

analysis and ciELISA characterization, the five mutants can be categorized into two groups. The first group comprising scFvC4A9H1_mut1, mut2, and mut3 exhibited similar cross-reactivity profiles to 20 FQs (Table 1). Importantly, compared with wild-type scFvC4A9H1, the IC_{50} of these three mutants to SAR, DIF and TRO decreased about 10-fold while the IC_{50} values to other FQs only changed slightly. In all these three scFv mutants, the substitutions of wild-type amino acids with smaller ones (Gly or Ala) were observed at position H95, H96, and H98, and no mutation was observed at SerH97 and TyrH99. The second group comprising scFvC4A9H1_mut4 and mut5 showed dramatically decreased affinity to FLU, PAZ and PRU, in spite to the increased affinity to SAR and its analogues. The mutations observed at H95, H96, and H98 in both scFv mutants were almost the same as in group 1: all the relatively large amino acids at these positions in the wild-type scFvC4A9H1 were substituted with smaller ones (Gly, Ser, or Ala). Different to the first group, two additional mutations SerH97Arg and TyrH99Gln were observed in scFvC4A9H1_mut4 and mut5.

As discussed above, our NOR-scFv and SAR-scFv docking models suggested that the amino acids from H95 to H99 formed the bottom surface of the binding groove to piperazinyl at FQs position 7, and this region were considered responsible for the hundred-fold difference between IC_{50} values of wild-type scFv to NOR and SAR. In NOR docked model, SerH97 formed a hydrogen bond with distal nitrogen atom of piperazinyl, which was the primary contributor to the recognition and binding of piperazinyl. However, in the SAR docked model, the increased distance between SerH97 and distal nitrogen atom prevented the formation of the same hydrogen bond. Indeed, biased random mutations introduced to this region improved the recognition of SAR and its analogues and ensured retaining affinity to the other FQs. In all five selected mutants, observed substitutions of AlaH95, LeuH96 and LeuH98 with smaller amino acids (Ala, Gly, or Ser) indicated that this compact N-terminal corner of more flexibility in CDR H3 was favorable in binding of SAR. In group 1 where the mutants showed the best cross-reactivity profile to all FQs and 10-fold improved affinity to SAR, no mutations was founded at SerH97 and TyrH99, which suggested that these two amino acids play a very important role in recognition of SAR. Based on these observed mutations and ciELISA results, we concluded that the flexible N-terminal corner structure in CDR H3 made the SAR molecule, especially the piperazinyl group, fitting more accurately and closer into the binding sites. Thus, in presence of SerH97, the stronger short contacts and the same hydrogen bond as NOR docked model between piperazinyl and mutants CDR H3 formed Although the other retained amino acid TyrH99 from wild-type scFvC4A9H1 was located in the outer surface of the VH domain and did not contact the hapten directly, the hydrogen bond between it and AsnL34 was considered important for maintenance of the VH-VL dimer. All these CDR H3 mutations seem favorable to recognize and bind the piperazinyl of FQs, and explained the improved affinity to SAR and its analogues without losing the affinity to the other FQs possessing a piperazinyl group at position 7. However, the change of the CDR H3 conformation caused by these mutations disturbed the interaction between the scFv and ring A or ring B in some way, which resulted in a 2-fold increase of IC_{50} to FLU, PAZ, and PRU not contain a piperazinyl group at position 7. A similar but much more significant increase in IC_{50} values to these "no piperazinyl" FQs was observed in mutants of the second group. In the second group, the important mutations SerH97Arg and TyrH99Gln also led to the increased affinity to SAR and its analogues by the potential hydrogen bond or other interactions formed

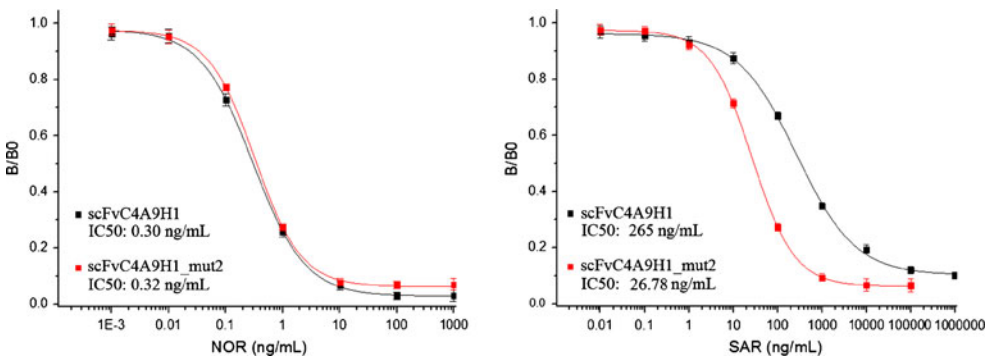

Fig. 5 The representative ciELISA standard curves

between piperazinyl and its binding site. However, in contrast to Ser, the intensely positively charged and relatively large side chain of Arg must have strongly affect the contacts between other FQs common structures (rings A and B) and binding sites, or possibly even lead to completely different interactions between FQ molecules and mutated binding site, as indicated by the increased IC_{50} values of the second mutants group to all FQs, except SAR and its analogues. As for the other mutation TyrH99Gln, because of the potential hydrogen bonding between GlnH99 and AsnL34, TyrH99Gln only brought a very limited effect to the binding site conformation.

Conclusions

The scFvC4A9H1 against FQs was successfully prepared from mAbC49H1. For the first time, homology modeling and docking study were used to investigate and demonstrate the interactions between FQs and scFvC4A9H1. Based on molecular modeling research, five N-terminal amino acids in the CHR H3 were identified as target positions for random mutations to broaden the binding of scFvC4A9H1 to SAR, DIF and TRO. A site-directed mutagenesis phage library was designed and constructed to develop an anti-FQs generic scFv with improved affinity to SAR and its analogues. After five rounds panning combined with competitive elution, five scFv mutants were isolated from the library. The best scFv molecule obtained in our study, scFvC4A9H1_mut2, showed 10-fold improved affinity to SAR and its analogues while the affinity to other FQs was fully inherited from wild-type scFvC4A9H1.

Acknowledgments We thank Prof. Andreas Plückthun for providing the plasmids pAK100 and pJB33. This study is financial supported by the National Natural Science Foundation of China (30830082), Joint Chinese–German Junior Research Group on Biotechnology (2009DFA32330), the Program for Cheung Kong Scholars and Innovative Research Team in University of China (IRT0866), Study of the molecular mechanisms of recombinant ScFv antibodies recognizing multi-veterinary drug (31172361), and Russia–China international cooperation program (2011DFR30470)

References

1. Winter RW, Kelly JX, Smilkstein MJ, Dodean R, Hinrichs D, Riscoe MK (2008) Antimalarial quinolones: synthesis, potency, and mechanistic studies. Exp Parasitol 118(4):487–497. doi:10.1016/j.exppara.2007.10.016
2. Schneider MJ, Braden SE, Reyes-Herrera I, Donoghue DJ (2007) Simultaneous determination of fluoroquinolones and tetracyclines in chicken muscle using HPLC with fluorescence detection. J Chromatogr B Anal Technol Biomed Life Sci 846(1–2):8–13. doi:10.1016/j.jchromb.2006.08.005
3. Hassouan MK, Ballesteros O, Taoufiki J, Vilchez JL, Cabrera-Aguilera M, Navalon A (2007) Multiresidue determination of quinolone antibacterials in eggs of laying hens by liquid chromatography with fluorescence detection. J Chromatogr B Anal Technol Biomed Life Sci 852(1–2):625–630. doi:10.1016/j.jchromb.2006.12.039
4. Zeng Z, Dong A, Yang G, Chen Z, Huang X (2005) Simultaneous determination of nine fluoroquinolones in egg white and egg yolk by liquid chromatography with fluorescence detection. J Chromatogr B Anal Technol Biomed Life Sci 821(2):202–209. doi:10.1016/j.jchromb.2005.05.007
5. Bogialli S, D'Ascenzo G, Di Corcia A, Laganà A, Tramontana G (2009) Simple assay for monitoring seven quinolone antibacterials in eggs: extraction with hot water and liquid chromatography coupled to tandem mass spectrometry: laboratory validation in line with the European Union Commission Decision 657/2002/EC. J Chromatogr A 1216(5):794–800. doi:10.1016/j.chroma.2008.11.070
6. Xiao Y, Chang H, Jia A, Hu J (2008) Trace analysis of quinolone and fluoroquinolone antibiotics from wastewaters by liquid chromatography–electrospray tandem mass spectrometry. J Chromatogr A 1214(1–2):100–108. doi:10.1016/j.chroma.2008.10.090
7. Ye Z, Weinberg HS, Meyer MT (2006) Trace analysis of trimethoprim and sulfonamide, macrolide, quinolone, and tetracycline antibiotics in chlorinated drinking water using liquid chromatography electrospray tandem mass spectrometry. Anal Chem 79 (3):1135–1144. doi:10.1021/ac060972a
8. Herrera-Herrera AV, Ravelo-Perez LM, Hernandez-Borges J, Afonso MM, Palenzuela JA, Rodriguez-Delgado MA (2011) Oxidized multi-walled carbon nanotubes for the dispersive solid-phase extraction of quinolone antibiotics from water samples using capillary electrophoresis and large volume sample stacking with polarity switching. J Chromatogr A 1218(31):5352–5361. doi:10.1016/j.chroma.2011.06.031
9. Liu YM, Jia YX, Tian W (2008) Determination of quinolone antibiotics in urine by capillary electrophoresis with chemiluminescence detection. J Sep Sci 31(21):3765–3771. doi:10.1002/jssc.200800373
10. Lara FJ, Garcia-Campana AM, Ales-Barrero F, Bosque-Sendra JM, Garcia-Ayuso LE (2006) Multiresidue method for the determination of quinolone antibiotics in bovine raw milk by capillary electrophoresis-tandem mass spectrometry. Anal Chem 78 (22):7665–7673. doi:10.1021/ac061006v
11. Juan-Garcia A, Font G, Pico Y (2006) Determination of quinolone residues in chicken and fish by capillary electrophoresis–mass spectrometry. Electrophoresis 27(11):2240–2249. doi:10.1002/elps.200500868
12. Okerman L, Noppe H, Cornet V, De Zutter L (2007) Microbiological detection of 10 quinolone antibiotic residues and its application to artificially contaminated poultry samples. Food Addit Contam 24(3):252–257. doi:10.1080/02652030600988020
13. Van Coillie E, De Block J, Reybroeck W (2004) Development of an indirect competitive ELISA for flumequine residues in raw milk using chicken egg yolk antibodies. J Agric Food Chem 52 (16):4975–4978. doi:10.1021/jf049593d
14. Haasnoot W, Gercek H, Cazemier G, Nielen MW (2007) Biosensor immunoassay for flumequine in broiler serum and muscle. Anal Chim Acta 586(1–2):312–318. doi:10.1016/j.aca.2006.10.003
15. Huet A-C, Charlier C, Tittlemier SA, Singh G, Benrejeb S, Delahaut P (2006) Simultaneous determination of (Fluoro)quinolone antibiotics in kidney, marine products, eggs, and muscle by enzyme-linked immunosorbent assay (ELISA). J Agric Food Chem 54(8):2822–2827. doi:10.1021/jf052445i
16. Kato M, Ihara Y, Nakata E, Miyazawa M, Sasaki M, Kodaira T, Nakazawa H (2007) Development of enrofloxacin ELISA using a monoclonal antibody tolerating an organic solvent with broad cross-reactivity to other newquinolones. Food Agric Immunol 18 (3–4):179–187

17. Li Y, Ji B, Chen W, Liu L, Xu C, Peng C, Wang L (2008) Production of new class-specific polyclonal antibody for determination of fluoroquinolones antibiotics by indirect competitive ELISA. Food Agric Immunol 19(4):251–264
18. Wang Z, Zhu Y, Ding S, He F, Beier RC, Li J, Jiang H, Feng C, Wan Y, Zhang S, Kai Z, Yang X, Shen J (2007) Development of a monoclonal antibody-based broad-specificity ELISA for fluoroquinolone antibiotics in foods and molecular modeling studies of cross-reactive compounds. Anal Chem 79(12):4471–4483. doi:10.1021/ac070064t
19. Cao L, Kong D, Sui J, Jiang T, Li Z, Ma L, Lin H (2009) Broad-specific antibodies for a generic immunoassay of quinolone: development of a molecular model for selection of haptens based on molecular field-overlapping. Anal Chem 81(9):3246–3251. doi:10.1021/ac802403a
20. Leivo J, Chappuis C, Lamminmaki U, Lovgren T, Vehniainen M (2011) Engineering of a broad-specificity antibody: detection of eight fluoroquinolone antibiotics simultaneously. Anal Biochem 409(1):14–21. doi:10.1016/j.ab.2010.09.041
21. Sambrook J, Russell DW (2001) Molecular cloning: a laboratory manual, vol 2. Cold Spring Harbor Laboratory Press, Cold Spring Harbor, New York
22. Goodfriend TL, Levine L, Fasman GD (1964) Antibodies to bradykinin and angiotensin: a use of carbodiimides in immunology. Science 144:1344–1346
23. Schaefer JV, Plückthun A (2010) Improving expression of scFv fragments by co-expression of periplasmic chaperones. In: Kontermann, R; Dübel, S. (eds) Antibody Engineering. Springer, Berlin, pp 345–361
24. Xiao T, Takagi J, Coller BS, Wang JH, Springer TA (2004) Structural basis for allostery in integrins and binding to fibrinogen-mimetic therapeutics. Nature 432(7013):59–67
25. Mizutani R, Miura K, Nakayama T, Shimada I, Arata Y, Satow Y (1995) Three-dimensional structures of the Fab fragment of murine N1G9 antibody from the primary immune response and of its complex with (4-hydroxy-3-nitrophenyl) acetate. J Mol Biol 254 (2):208–222
26. Pozharski E, Wilson MA, Hewagama A, Shanafelt AB, Petsko G, Ringe D (2004) Anchoring a cationic ligand: the structure of the Fab fragment of the anti-morphine antibody 9B1 and its complex with morphine. J Mol Biol 337(3):691–697
27. Spassov VZ, Yan L, Flook PK (2007) The dominant role of side-chain backbone interactions in structural realization of amino acid code. ChiRotor: a side-chain prediction algorithm based on side-chain backbone interactions. Protein Science: A Publication of the Protein Society 16(3):494–506. doi:10.1110/ps.062447107
28. Wang Z, Raifu M, Howard M, Smith L, Hansen D, Goldsby R, Ratner D (2000) Universal PCR amplification of mouse immunoglobulin gene variable regions: the design of degenerate primers and an assessment of the effect of DNA polymerase 3′ to 5′ exonuclease activity. J Immunol Methods 233(1–2):167–177
29. Krebber A, Bornhauser S, Burmester J, Honegger A, Willuda J, Bosshard HR, Pluckthun A (1997) Reliable cloning of functional antibody variable domains from hybridomas and spleen cell repertoires employing a reengineered phage display system. J Immunol Methods 201(1):35–55
30. Rohatgi S, Ganju P, Sehgal D (2008) Systematic design and testing of nested (RT-)PCR primers for specific amplification of mouse rearranged/expressed immunoglobulin variable region genes from small number of B cells. J Immunol Methods 339(2):205–219. doi:10.1016/j.jim.2008.09.017
31. Honegger A, Pluckthun A (2001) The influence of the buried glutamine or glutamate residue in position 6 on the structure of immunoglobulin variable domains. J Mol Biol 309(3):687–699. doi:10.1006/jmbi.2001.4664
32. Bothmann H, Pluckthun A (1998) Selection for a periplasmic factor improving phage display and functional periplasmic expression. Nat Biotechnol 16(4):376–380. doi:10.1038/nbt0498-376
33. Kabat EA (1991) Sequences of proteins of immunological interest, vol 3. US Dept. of Health and Human Services, Public Health Service, National Institutes of Health
34. Schier R, McCall A, Adams GP, Marshall KW, Merritt H, Yim M, Crawford RS, Weiner LM, Marks C, Marks JD (1996) Isolation of picomolar affinity anti-*c*-erbB-2 single-chain Fv by molecular evolution of the complementarity determining regions in the center of the antibody binding site. J Mol Biol 263(4):551–567. doi:10.1006/jmbi.1996.0598
35. Schier R, Balint RF, McCall A, Apell G, Larrick JW, Marks JD (1996) Identification of functional and structural amino-acid residues by parsimonious mutagenesis. Gene 169(2):147–155
36. Lou J, Marks JD (2010) Affinity Maturation by Chain Shuffling and Site Directed Mutagenesis. Antibody Engineering. In: Kontermann R, Dübel S (eds). Springer, Berlin, pp 377–396. doi:10.1007/978-3-642-01144-3_25
37. Schier R, Bye J, Apell G, McCall A, Adams GP, Malmqvist M, Weiner LM, Marks JD (1996) Isolation of high-affinity monomeric human anti-*c*-erbB-2 single chain Fv using affinity-driven selection. J Mol Biol 255(1):28–43